2002

Dynamic Equilibrium between Coupled and Uncoupled Modes of a Neuronal Glutamate Transporter

Lars Borre

Michael Kavanaugh

Baruch I. Kanner

THE JOURNAL OF BIOLOGICAL CHEMISTRY
Vol. 277, No. 16, Issue of April 19, pp. 13501–13507, 2002
Printed in U.S.A.

Dynamic Equilibrium between Coupled and Uncoupled Modes of a Neuronal Glutamate Transporter*

Received for publication, November 13, 2001, and in revised form, January 30, 2002
Published, JBC Papers in Press, January 31, 2002, DOI 10.1074/jbc.M110861200

Lars Borre‡§, Michael P. Kavanaugh¶, and Baruch I. Kanner‡‖

From the ‡Department of Biochemistry, Hadassah Medical School, The Hebrew University, P. O. Box 12272, Jerusalem 91120, Israel and ¶The Vollum Institute, Oregon Health Sciences University, Portland, Oregon 97201

In the brain, the neurotransmitter glutamate is removed from the synaptic cleft by (Na^+ + K^+)-coupled transporters by an electrogenic process. Moreover, these transporters mediate a sodium- and glutamate-dependent uncoupled chloride conductance. In contrast to the wild type, the uptake of radiolabeled substrate by the I421C mutant is inhibited by the membrane-impermeant [2-(trimethylammonium)ethyl]methanethiosulfonate and also by other sulfhydryl reagents. In the wild-type and the unmodified mutant, substrate-induced currents are inwardly rectifying and reflect the sum of the coupled electrogenic flux and the anion conductance. Remarkably, the I421C mutant modified by sulfhydryl reagents exhibits currents that are nonrectifying and reverse at the equilibrium potential for chloride. Strikingly, almost 10-fold higher concentrations of D-aspartate are required to activate the currents in the modified mutant as compared with untreated I421C. Under conditions in which only the coupled currents are observed, the modified mutant does not exhibit any currents. However, when the uncoupled current is dominant, sulfhydryl reagents cause >4-fold stimulation of this current. Thus, the modification of the cysteine introduced at position 421 impacts the coupled but not the uncoupled fluxes. Although both fluxes are activated by substrate, they behave as independent processes that are in dynamic equilibrium.

The major excitatory neurotransmitter in the brain is glutamate. Transporters remove the transmitter from the synaptic cleft so that its extracellular concentrations are maintained below neurotoxic levels (1–5). Moreover, glutamate transporters play an important role in limiting the duration of synaptic excitation (6–9). Glutamate transport is an electrogenic process (10–12) involving cotransport with sodium and hydrogen ions followed by countertransport of potassium (13–15). The stoichiometry of the process has been determined to be $3Na^+$:$1H^+$:$1K^+$:glutamate (3, 16).

The five known eukaryotic glutamate transporters, glutamate transporter-1 (17), glutamate/aspartate transporter-1 (18), EAAC-1 (19),[1] EAAT-4 (20), and EAAT-5 (21), have an overall identity of approximately 50%. The homology is significantly higher in the carboxyl-terminal half. Glutamate transporters have a non-conventional topology containing two reentrant loops, two transmembrane domains, as well as an outward facing hydrophobic linker region (22–24), although there remains some controversy over some of the features of this topology (25). Two adjacent amino acid residues, tyrosine 403 and glutamate 404, of glutamate transporter-1 located in transmembrane domain 7 and conserved in all other glutamate transporters are required for potassium binding (15, 26). Two other residues located in reentrant loop II and transmembrane domain 7, respectively, have been found to be determinants of sodium specificity (27, 28). Arginine 447 of the EAAC-1 transporter located in transmembrane domain 8 and also fully conserved in the other glutamate transporters appears to be a determinant for the binding of the γ-carboxyl group of glutamate and is also important for potassium interaction (29).

In addition to the ion-coupled glutamate translocation, glutamate transporters mediate a thermodynamically uncoupled chloride flux. It is activated by two of the molecules they transport, sodium and glutamate (20, 30). This indicates the existence of a tight link between gating of the anion conductance and permeation of glutamate. It has been suggested that this capacity for enhancing chloride permeability may serve to offset the depolarization that occurs during glutamate transport (20). In a very recent study (28), we have reported that in EAAC-1, lithium can replace sodium in the coupled uptake but not in its capacity to gate the glutamate-dependent anion conductance. This finding suggests that the conformation gating the anion conductance may be different from that during substrate translocation. If this idea is correct, it should be possible to selectively perturb one of the two fluxes mediated by the glutamate transporters.

We have engineered externally accessible cysteines into EAAC-1 with the aim of introducing fluorescent maleimides to monitor conformational changes during transport. An analysis of one of the mutants with a cysteine residue introduced in the hydrophobic linker region revealed that the coupled uptake in this mutant is very sensitive to sulfhydryl reagents. Strikingly, the substrate-induced anion conductance is not affected at all under these conditions. We have exploited the sulfhydryl-modified mutant to reveal novel properties of the substrate-gated anion-conducting state and its relation to the coupled transport cycle.

* This work was supported by Grant 9900123 from the United States-Israel Binational Science Foundation, the European Community Training and Mobility of Researcher Program, Grant NS 16708 from the NINDS, National Institutes of Health, the Federal Ministry of Education, Science, Research and Technology and its International Bureau at the Deutsches Zentrum für Luft and Raumfahrt, and the Bernard Katz Minerva Center for Cellular Biophysics. The costs of publication of this article were defrayed in part by the payment of page charges. This article must therefore be hereby marked "*advertisement*" in accordance with 18 U.S.C. Section 1734 solely to indicate this fact.

§ Recipient of a Danish Research Agency Fellowship.
‖ To whom correspondence should be addressed. Tel.: 972-2-675-8506; Fax: 972-2-675-7379; E-mail: kannerb@cc.huji.ac.il.

[1] The abbreviations used are: EAAC-1, excitatory amino acid carrier-1; EAAT, excitatory amino acid transporter; MTSET, [2-(trimethylammonium)ethyl]methanethiosulfonate; DTT, dithiothreitol; I/V, current/voltage relation.

EXPERIMENTAL PROCEDURES

Generation and Subcloning of Mutants—The rabbit glutamate transporter EAAC-1 (19) with nine histidines added (29) in the vector pBluescriptSK(−) (Stratagene) was used as a parent for site-directed mutagenesis as described previously (31, 32). Restriction enzymes *Pin*AI and *Pfl*MI were used to subclone the mutations into the construct containing the His-tagged wild-type EAAC-1 residing in either pBluescriptSK(−) or in pOG_2 (29). pOG_2 is an oocyte expression vector containing a 5′-untranslated *Xenopus* β-globin sequence and a 3′-poly(A) signal. The coding and non-coding strands were sequenced between the above two restriction sites.

Expression and Uptake in HeLa Cells—HeLa cells were cultured in supplemented Dulbecco's modified Eagle's medium (Biological Industries), infected with a recombinant vaccinia/T7 virus vTF_{7-3} (33), and transfected with 0.5 μg of DNA/well using LipofectAMINE (2 μg/well) (Roche Molecular Biochemicals), and D-[2,3-^{3}H]aspartic acid uptake was measured as described previously (28). For experiments using the sulfhydryl reagent MTSET (Toronto Research Chemicals), culture medium was removed, and the cells were washed twice with 1 ml of choline uptake solution (sodium replaced with equimolar choline) and then incubated with 200 μl of uptake solution containing 500 μM MTSET for 2 min. Cells were washed again twice in 1 ml of choline uptake solution (37 °C) before the 10-min uptake assay was initiated by adding 200 μl of radioactive sodium uptake solution at 37 °C. Cells that did not receive MTSET were subjected to the same incubation and washing procedures. From dose-response experiments, the concentration of MTSET giving half-maximal inhibition was determined to be 5 μM (data not shown). 100–5000 × this concentration has been used on HeLa cells and oocytes in initial experiments to rule out the possibility that MTSET reacts with wild-type EAAC1.

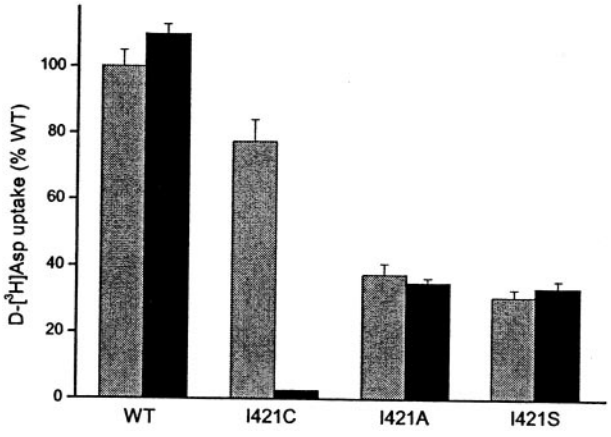

FIG. 1. **Effect of MTSET on D-[^{3}H]aspartate uptake in HeLa cells expressing substitution mutants at position 421 of EAAC-1.** Aspartate uptake (10 min at 37 °C) in cells incubated with (*dark bars*) or without (*gray bars*) 500 μM MTSET was measured as described under "Experimental Procedures," using 2 μCi/ml D-[2,3-^{3}H]aspartate (18 Ci/mmol). The results are expressed as percent activity of the untreated wild-type EAAC-1 and are means ± S.E. of 6–9 determinations.

cRNA Transcription, Injection, and Oocyte Preparation—Capped run-off cRNA transcripts were made from transporter constructs in pOG_2 and linearized with *Sac*I using mMessage mMachine (Ambion), and *Xenopus laevis* oocytes were prepared using collagenase type 1A (Sigma) or Blendzyme 3 (Roche Molecular Biochemicals) and injected as described previously (28). Oocytes were maintained either in modified Barth's saline solution (88 mM NaCl, 1 mM KCl, 1 mM $MgSO_4$, 2.4 mM $NaHCO_3$, 1 mM $CaCl_2$, 0.3 mM $Ca(NO_3)_2$, 10 mM HEPES, pH 7.5, with freshly added 2 mM sodium pyruvic acid and 0.5 mM theophylline) supplemented with 10,000 units/liter of penicillin, 10 mg/liter streptomycin, and 50 mg/liter gentamycin or in ND96-recording solution (see below) supplemented with 1.5% heat-inactivated horse serum, 0.5 mM theophylline, and 2.5 mM pyruvic acid.

Oocyte Electrophysiology—Currents were measured from *X. laevis* oocytes using conventional two-electrode voltage clamp recording as described previously (28). Penetrated oocytes were gravity-perfused with ND96-recording solution (96 mM NaCl, 2 mM KCl, 1.8 mM $CaCl_2$, 1 mM $MgCl_2$, 5 mM HEPES-hemisodium, pH 7.5). Sodium chloride and HEPES-hemisodium were replaced with equimolar choline chloride and free acid HEPES or replaced with equimolar lithium chloride and free acid HEPES in sodium replacement experiments (pH was adjusted to pH 7.5 with Tris-OH in these solutions). In experiments using the highly permeant thiocyanate anion (Fig. 6), 2 mM KCl was replaced by 20 mM KSCN, and the sodium chloride concentration was varied by replacing NaCl with equimolar choline chloride. In these experiments, the extracellular grounding electrode was placed in 2 M KCl and connected to the recording chamber with an agar/2 M KCl bridge. Before applying either of the sulfhydryl reagents, MTSET (Toronto Research Chemicals) or β-maleimidopropionic acid (Sigma), the flow was stopped, and the reagent was added directly into the bath under voltage clamp. Before applying the reducing agent, 1,4-dithiothreitol (DTT), directly into the bath, the oocyte was unclamped, grounding electrode was removed, and the flow was stopped. MTSET and/or DTT was allowed to react for 2 min followed by an ~10-min washout (in initial experiments using higher MTSET and DTT concentrations the washout time was 20 min). The net current was measured before MTSET application, after MTSET application, and after DTT application in that order. Both the MTSET and the β-maleimidopropionic acid stock solutions were made in the recording solution to which it was added (in the case of maleimide, pH was adjusted to 7.5 with NaOH) and kept on ice for up to 2 h, and the DTT was made in 1 mM sodium acetate, pH 5.2. The final concentrations in the bath of MTSET and DTT were 2.5–25 and 50 mM, respectively, in initial experiments and later concentrations were 1 and 10 mM, respectively, as estimated from the measured chamber volume in the presence of an oocyte. Unless stated otherwise, oocytes were perfused in recording solution with or without 1 mM D-aspartate or L-aspartate.

Data Analysis—Data have been normalized to account for variability in expression level within and between different oocyte batches. Steady-

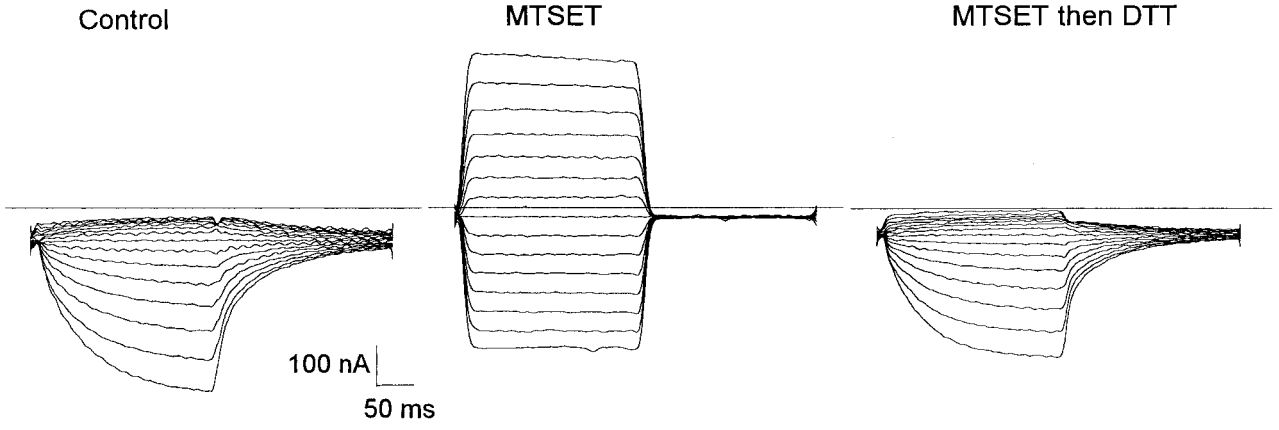

FIG. 2. **Net currents in sodium medium mediated by D-aspartate in I421C-EAAC-1 transporters.** Currents recorded in the absence of D-aspartate during 250-ms voltage pulses from −100 to +40 mV subtracted from currents recorded during superfusion of 1 mM D-aspartate (net current). The prepulse potential was −25 mV. *Horizontal line* indicates zero current level. The net currents were measured before MTSET application (*Control*), after MTSET application (*MTSET*), and after MTSET application followed by DTT (*MTSET then DTT*). MTSET was used at 5 mM, but similar results were obtained with 1 mM used on other oocytes. DTT was used at 10 mM. A typical experiment is shown (n = 10).

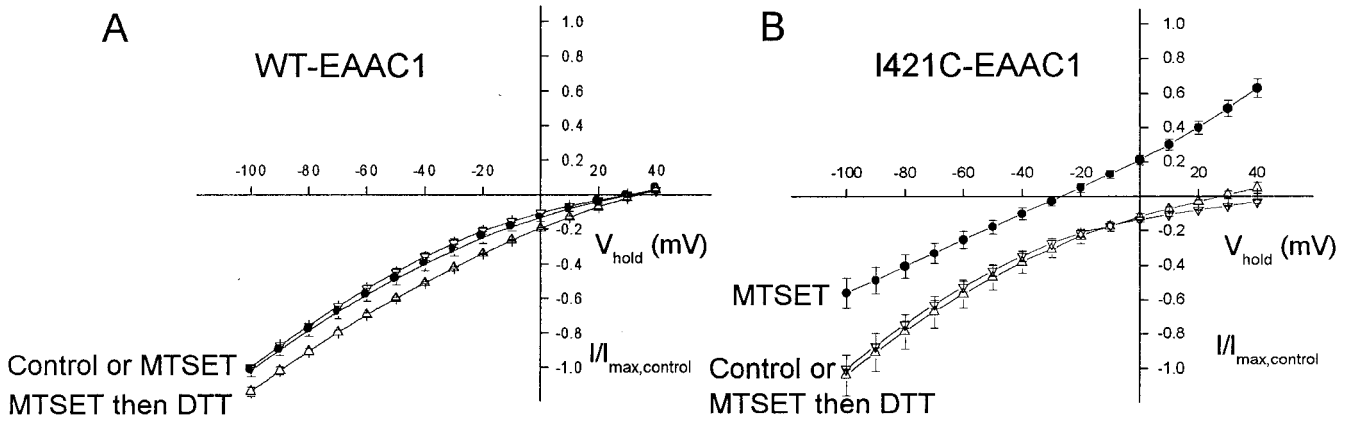

FIG. 3. **Voltage dependence of steady-state net currents before and after MTSET treatment.** Voltage dependence of net D-aspartate currents in oocytes expressing wild-type EAAC-1 (*A*) or I421C-EAAC-1 (*B*) before MTSET, after MTSET application, and after MTSET application followed by DTT as indicated in the figure (n = 10). Net currents at −100 mV ranged from −500 to −1000 nA (*A*) and from −300 to −620 nA (*B*).

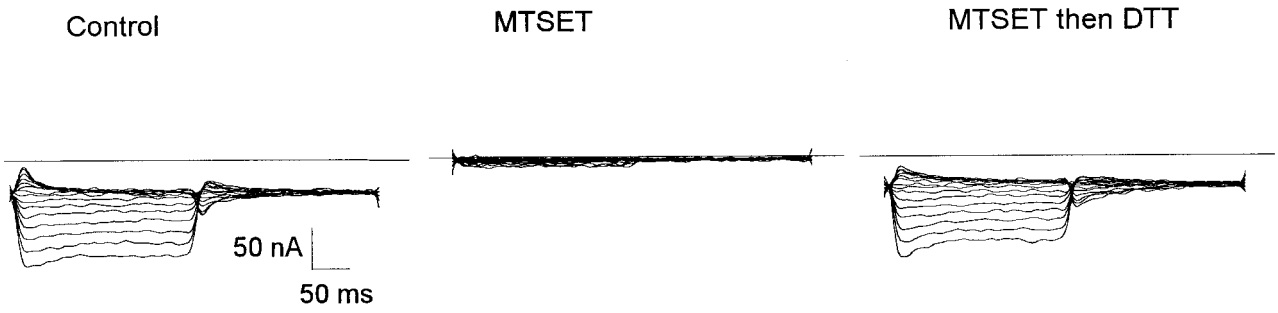

FIG. 4. **Net currents in lithium medium mediated by L-aspartate in I421C-EAAC-1 transporters.** Currents recorded in the absence of L-aspartate during 250-ms voltage pulses from −100 to +40 mV were subtracted from currents during superfusion of 1 mM L-aspartate. The application order of MTSET (1 mM) and DTT (10 mM) was as described in the legend to Fig. 2. A typical experiment is shown (n = 6).

state net currents defined as ($I_{ND+D\text{-}Asp} - I_{ND}$) were analyzed using Clampfit6.05 and Origin6.1 (Microcal). The current-voltage relations shown were obtained by averaging the net currents at each holding potential from 218 to 248 ms. For representational purposes, the traces of the net currents shown in Figs. 2 and 4 have been low pass-filtered off-line using the boxcar algorithm (Clampfit). Concentrations of D-aspartate or sodium giving half-maximal currents (EC_{50}) were determined with the generalized Hill equation (28) using a fixed maximum current (I_{max}), and the determined EC_{50} and Hill number (n_H) were used to generate the curves shown. Residuals were minimized with the Levenberg-Marquehardt method. The build-in functions of Origin6.1 were used for statistical testing. Data are the means ± S.E. of 3–10 oocytes from 2–4 different batches.

RESULTS

Inhibition of D-[^{3}H]Aspartate Uptake in I421C by MTSET—HeLa cells expressing the I421C-EAAC-1 mutant exhibit similar rates of D-[^{3}H]aspartate uptake as those in which the wild type is expressed (Fig. 1). However, in contrast to the wild type, this uptake is almost fully inhibited by preincubation of the cells with 500 μM of the impermeant sulfhydryl reagent MTSET (Fig. 1). The introduction of a serine or an alanine residue at this position does not render EAAC-1 sensitive to MTSET (Fig. 1). These observations indicate that the inhibition of uptake in I421C-EAAC-1 is the result of the introduced cysteine and renders unlikely the possibility that the introduction of a cysteine at position 421 causes the transporter to expose an endogenous cysteine that could mediate the inhibition by the sulfhydryl reagent. When I421C-EAAC-1 is treated with a concentration of MTSET low enough (5 μM) to retain significant residual activity, the major impact is on maximal uptake (V_{max} = 66 ± 6% inhibition (n = 3)). The apparent affinity for substrate (K_m) is essentially unchanged (27 ± 5 and 25 ± 4 μM (n = 3)) for untreated and MTSET treated I421C, respectively. This finding indicates that the inactivation of uptake by MTSET is because of a progressive reduction of functional transporters.

Modification of the Substrate-gated Currents by Sulfhydryl Reagents—It is well established that in sodium-containing media, the addition of acidic amino acid substrates to oocytes expressing cloned glutamate transporters results in the activation of a current representing the sum of two currents. The first is a non-reversing inwardly rectifying current reflecting the coupled cycle, whereas the second is a reversing non-rectifying anion conductance that is thermodynamically uncoupled (20, 21, 30). The reversal potential of the combined current depends on the acidic amino acid substrate. L-Aspartate gives rise to the reversal at less positive potentials than L-glutamate and D-aspartate (28, 30). An analysis of the D-aspartate-induced currents of oocytes expressing I421C-EAAC-1 in the presence and absence of MTSET reveals a remarkable result. Instead of currents, which are inward at the range of membrane potentials tested (−100 mV to +40 mV), preincubation with 1 mM MTSET results in currents that are almost symmetrical around the holding potential of −25 mV (Fig. 2). The treatment of the MTSET-modified mutant transporters with dithiothreitol, which is expected to restore the cysteine at the 421 position, also restores the voltage dependence of the D-aspartate-induced currents (Fig. 2). Similar results have been obtained when L-aspartate-induced currents are monitored (data not shown). Other sulfhydryl reagents such as (2-aminoethyl)-methanethiosulfonate and β-maleimidopropionic acid modify the currents of I421C in a similar way as MTSET. As expected, DTT is able to restore the current modified by (2-aminoethyl)-methanethiosulfonate but not by β-maleimidopropionic acid (data not shown). Plotting the average current/voltage relation

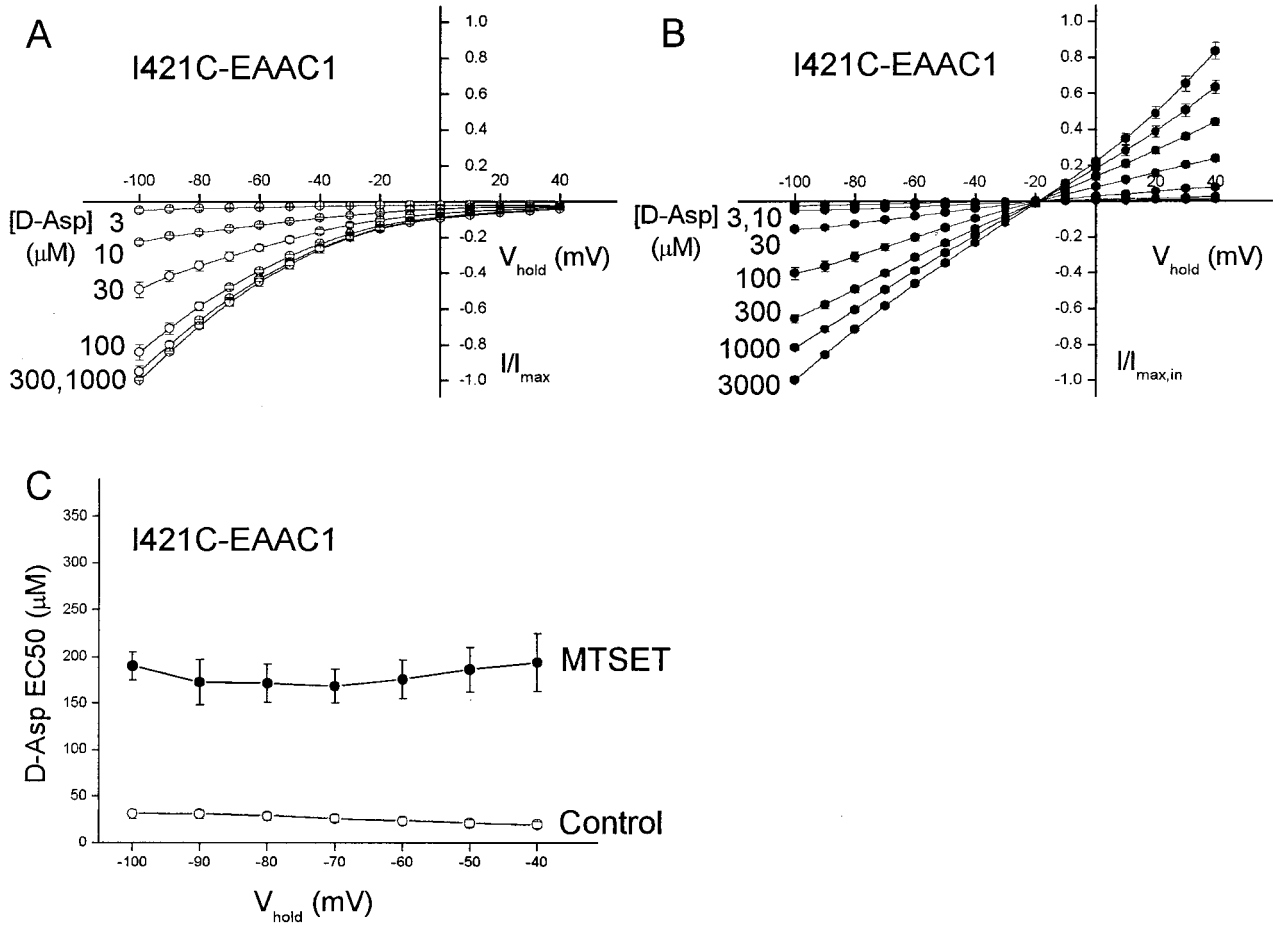

FIG. 5. **Concentration dependence of D-aspartate-dependent steady-state net currents in I421C-EAAC-1.** Voltage dependence of steady-state net currents at the indicated concentrations of D-aspartate before (*A*) and after treatment with 2.5 mM MTSET (*B*). The dependence of EC_{50}, determined from (*A*) and (*B*), on voltage is displayed in *C*. Net currents at −100 mV ranged from −260 to −460 nA at 1 mM D-aspartate (*A*) and from −330 to −460 nA at 3 mM D-aspartate (*B*). Data are means ± S.E. of three oocytes.

(I/V plot) of six oocytes shows that MTSET treatment of I421C changes the behavior of the substrate-induced currents from inwardly rectifying to ohmic. The currents observed after MTSET treatment reverse at −25 mV (Fig. 3*B*). DTT restores the inwardly rectifying currents (Fig. 3*B*). In contrast, the I/V relations of wild-type EAAC-1 are not affected by MTSET (Fig. 3*A*). It is of interest to note that the reversal potential of the D-aspartate-induced currents of the MTSET-treated I421C transporters is approximately −25 mV (Fig. 3*B*), very close to the reversal potential of chloride (30). Moreover, the I/V relation in this mutant is reminiscent of those in glutamate transporter-1 and EAAC-1 mutants, which are locked in the exchange mode (15, 26, 29) and therefore only exhibit the uncoupled chloride conductance.

Additional evidence supporting the idea that the currents observed with MTSET-modified I421C transporters solely represent the anion conductance is provided in Fig. 4. We have very recently found that in the presence of lithium, EAAC-1 transporters mediate the coupled current only (28). If the currents from MTSET-modified I421C solely are the result of the substrate-induced anion conductance, one would predict that in lithium medium no current will be observed at all. Because net D-aspartate currents in lithium medium are rather small, we have displayed the currents obtained with L-aspartate. The latter substrate gives rise to larger currents in lithium medium (28). As can be seen in Fig. 4, MTSET-treated I421C transporters do not exhibit any significant L-aspartate-induced currents in lithium medium. Again, the effect of MTSET can be reversed by DTT.

Characterization of the Substrate-gated Anion Conductance—The selective elimination of the coupled current in I421C by MTSET allows us to study the substrate-activated gating of the anion conductance in isolation from substrate translocation. One prediction is that the reversal potential of the current should be independent of the concentration of D-aspartate, but this would not be expected for the size of the current. Indeed, at increasing D-aspartate concentrations, the reversal potential remains the same (Fig. 5*B*). On the other hand, the size of the current representing the opening of more chloride channels increases with the increasing D-aspartate concentration (Fig. 5*B*). The dependence of the current of untreated I421C-EAAC1 transporters on the D-aspartate concentration is shown in Fig. 5*A*. It is inwardly rectifying and similar to that of wild-type EAAC-1 with or without MTSET treatment (data not shown). Also, the affinity of untreated I421C-EAAC-1 of ~25 μM is similar to that of the wild type with or without the sulfhydryl reagent (data not shown) (19). An analysis of the D-aspartate concentration dependence of the currents reveals that in MTSET-treated I421C, the apparent affinity for this substrate is lowered by almost 10 times as compared with the untreated mutant transporters (Fig. 5*C*). The Hill number for D-aspartate is not changed (Student's *t* test at the 0.05 significance level): 1.1 ± 0.1 and 1.2 ± 0.2 at −100 and +40 mV, respectively, before treatment and 0.9 ± 0.1 and 1.0 ± 0.2 after treatment with MTSET. In both cases the apparent affinity is voltage-independent, at least at negative potentials where a direct comparison is feasible (Fig. 5*C*).

We have taken advantage of the I421C mutant to address the

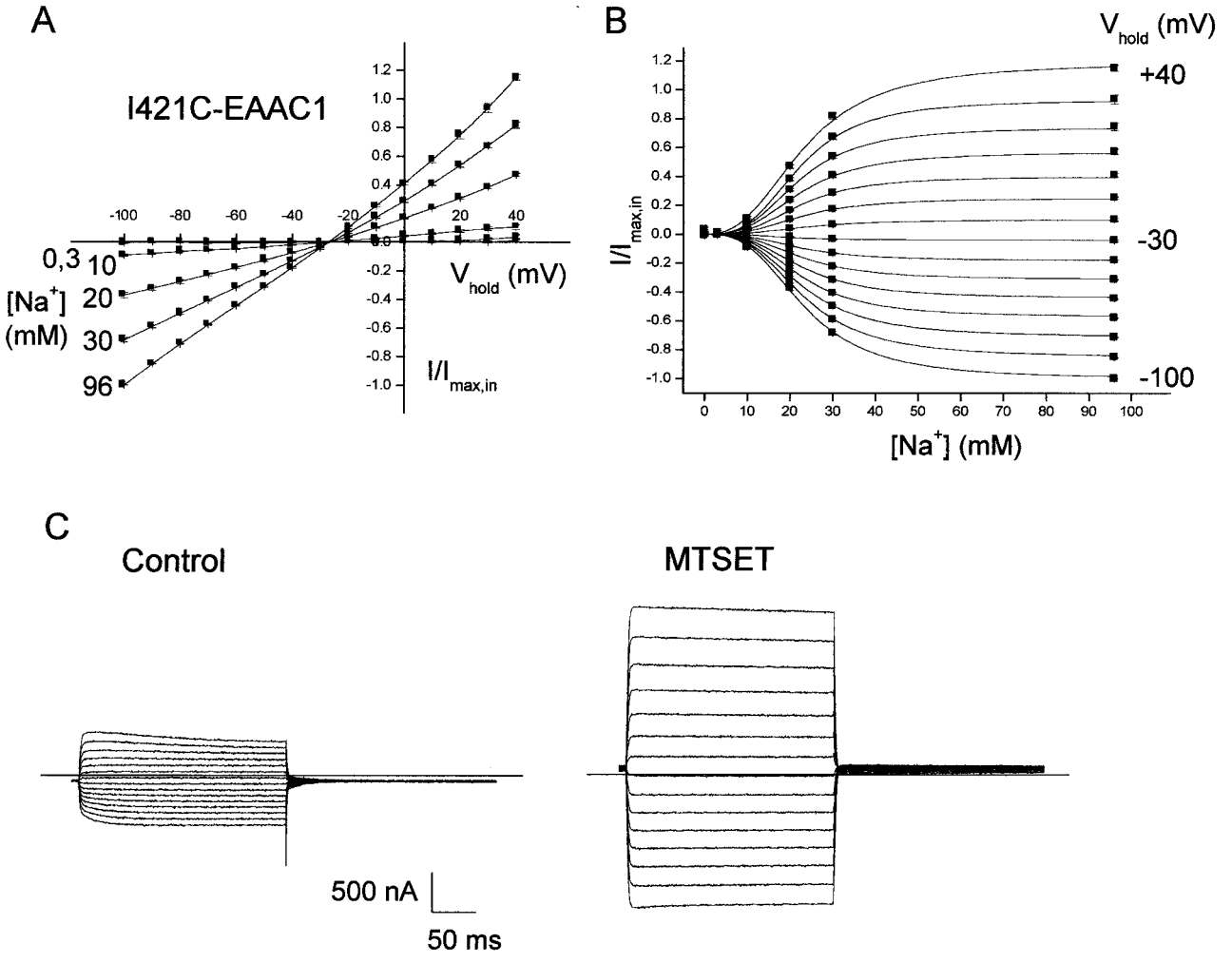

FIG. 6. **D-Aspartate steady-state net currents in I421C-EAAC1 in the presence of thiocyanate.** *A,* voltage dependence of D-aspartate (3 mM) steady-state net currents at the indicated sodium concentrations after treatment with 1 mM MTSET. *B,* sodium dependence of the net D-aspartate currents (data replotted from *A*). *C,* a typical experiment depicting the absolute currents at 96 mM sodium are shown before (*Control*) and after MTSET (*MTSET*) application. Absolute net currents in 96 mM sodium ranged from +370 to +1156 nA and from −380 to -2002 nA before MTSET application at +40 and −100 mV, respectively, and from +1551 to +4767 nA and from −818 to −4150 nA after MTSET application at +40 and −100 mV, respectively. Data are means ± S.E. of nine oocytes from four different batches. *Error bars* are smaller than the symbols.

question of whether (as is the case for coupled flux) multiple sodium ions are required to enable the substrate-gated anion conductance. To amplify the anion currents, 20 mM thiocyanate has been included in the perfusion medium, because its permeability is ~70-fold larger than that of chloride (30, 34). Fig. 6*A* illustrates the I/V plots of the D-aspartate (3 mM) net currents in MTSET-treated I421C-EAAC-1 transporters at varying sodium concentrations. Replotting these data *versus* the sodium concentration shows a cooperative behavior at all voltages tested (Fig. 6*B*). The sodium concentration, which gives rise to half-maximal currents, are similar (Student's *t* test at 0.05 significance level) at −100 mV and at +40 mV, namely 23.0 ± 0.4 and 23.3 ± 0.3 mM (n = 6), respectively. The same is true for the Hill numbers 3.0 ± 0.2 and 2.9 ± 0.1 at −100 and +40 mV, respectively (*t* test at 0.05 significance level). The data shown in Fig. 6, *A* and *B*, are normalized currents. An examination of the absolute net D-aspartate currents reveals the striking result that treatment with MTSET causes a marked stimulation of both inward and outward currents (Fig. 6*C*) as shown here at 96 mM sodium. At +40 and −100 mV, the increase is 4.43 ± 0.31- and 2.56 ± 0.17-fold, respectively (n = 6). This result indicates that when the anion conductance is the major component of the current, blocking the coupled cycle enables the transporter to reside longer in the conformation gating the anion conductance.

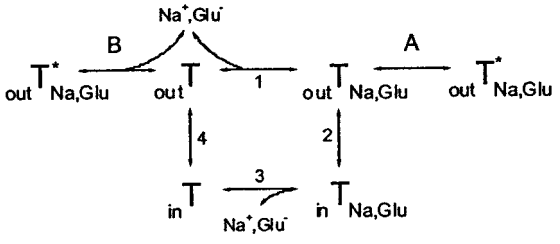

FIG. 7. **Possible interrelations between coupled and uncoupled pathways.** Depicted is the coupled pathway (*steps 1–4*) and the two possible entry routes into the anion-conducting state $_{out}T^*_{Na,Glu}$. Further details are given under "Discussion."

DISCUSSION

Our studies show that in I421C-EAAC-1 transporters, which otherwise behave identical to wild-type EAAC-1, sulfhydryl reagents abolish the uptake of D-[^{3}H]aspartate (Fig. 1) and modify the substrate-induced currents (Figs. 2 and 3). The characterization of those currents indicates that it is the cou-

pled flux that is affected. Whereas this flux is completely absent, the substrate-gated anion conductance is not affected by the sulfhydryl reagents (Figs. 2–4). We have used the mutant to study the anion conductance in isolation of the coupled current and obtained novel insights into the similarities and differences among these processes as well as their interrelation.

Possible pathways connecting coupled and uncoupled fluxes are shown in Fig. 7. The sodium-coupled glutamate translocation with the participating potassium ion and proton omitted for simplicity is represented by steps 1–4. After the binding of sodium and glutamate on the extracellular side (*step 1*), the translocation complex is formed. After translocation (*step 2*), the substrates are released on the intracellular side (*step 3*). The unloaded transporter binds potassium (not shown), and after translocation to the outside (*step 4*), potassium is released and the transporter is ready to start a new cycle. Because glutamate as well as the other acidic amino acid substrates gate the uncoupled anion conductance in a sodium-dependent manner, most models (34–37) propose a transition step of the outward-facing substrate-loaded transporter to an anion-conducting state, ${}_{out}T^*_{Na,Glu}$ (Fig. 7, *step A*). According to this scenario, the modification of the cysteine introduced at position 421 may be explained by a perturbation of either steps 2 or 3. HeLa cells expressing mutants locked in the exchange mode in which step 4 is impaired selectively still exhibit normal D-[^{3}H]aspartate uptake (15, 26). The complete inhibition of this uptake in I421C-EAAC-1 by MTSET (Fig. 1) renders selective inhibition of step 4 unlikely. The fact that the apparent affinity for D-aspartate to activate the anion conductance in I421C is almost 10-fold lower than that to activate the total current (Fig. 5*C*) can be easily accommodated by the alternative possibility depicted in Fig. 7, *step B*. According to this proposal, the anion-conducting state ${}_{out}T^*_{Na,Glu}$ can be reached without entering the coupled cycle. An inherent assumption is that the mutation has not somehow altered the apparent affinity of the uncoupled process for D-aspartate. Because the voltage dependence and the D-aspartate concentration dependence of the currents in the untreated mutant are identical to that of the wild type, it is likely that this assumption indeed is correct. Three sodium ions are translocated with glutamate in the coupled cycle (3, 16). Our study of the uncoupled flux indicates that this process also may require multiple sodium ions (Fig. 6, *A* and *B*). Therefore, one possibility is that two or three sodium ions bind to the transporter, and subsequently the sodium-bound transporter binds glutamate and enters either the coupled cycle or the anion-conducting state.

The role of the anion conductance has been postulated to counteract the depolarization caused by excessive glutamate flux (20). At high extracellular glutamate levels, the magnitude of this depolarization caused by the coupled process could be relatively large. Under these conditions, glutamate is likely to saturate the activation site of the anion conductance. Thus, at the same time, the influx of chloride will be activated, and this is expected to limit the depolarization. It is of interest that sulfhydryl modification of I421C also abolishes substrate-sensitive transient currents (Fig. 2). These transients probably represent voltage-dependent conformational changes associated with the coupled transport cycle but not those occurring during gating of the anion conductance.

The idea that the activation of the anion conductance is separate from that of the coupled transport (Fig. 7, *step B*) is in harmony with several recent independent lines of evidence. Kinetic experiments indicate that the onset of the uncoupled current is delayed compared with that of the coupled current (35–37), and the two exhibit different pH profiles (38) and cation specificities (28). Furthermore, it has been found that Zn^{2+} selectively perturbs the two processes. In the EAAT-1 transporter (the human homologue of glutamate/aspartate transporter-1), Zn^{2+} was found to inhibit the coupled but not the uncoupled current (39), and the reverse is true for EAAT-4 (40).

The scheme shown in Fig. 7 indicates that regardless of which of the two events in fact takes place, the steps of the coupled flux should be in dynamic equilibrium with the conformation gating the anion conductance. Selective blockade of the coupled cycle at either step 2 or step 3 is expected to increase the probability of entering the anion-gating conformation. The experiments shown in Figs. 2 and 6 support this idea. Upon modification of I421C with MTSET, the net outward D-aspartate currents emerge at positive potentials (Fig. 2). Before the addition of the sulfhydryl reagent, the current due to the coupled flux, which is inward even at +40 mV, is almost balanced by the outward current, which reflects the substrate-gated anion conductance (30). Selective elimination of the coupled current by sulfhydryl reagents reveals the outward anion current. In the presence of the highly permeable thiocyanate, the contribution of the anion conductance to the total current is markedly increased. At positive potentials, this conductance becomes the major component of the total current even before the addition of MTSET (30, 34–36). The result of the sulfhydryl modification is >4-fold stimulation of the anion-current (Fig. 6*C*) because of the enhanced probability of entering the conformation gating the anion conductance. At potentials more negative than the reversal potential, the stimulation of the inward current after MTSET treatment is approximately 2.5-fold, because two events now take place. The coupled current, which contributes significantly to the inward current, is inhibited at the same time as the anion current is stimulated.

Even though we have obtained new functional insights into coupled glutamate translocation and substrate-gated anion conductance, the structural basis of their possible interrelations remains unclear. Our observations that the modification of a cysteine residue introduced in the hydrophobic linker region selectively inhibits coupled flux suggest that this region may be less important for the activation of the anion conductance. It has been suggested that the same translocation pathway is used for both processes (30). An alternative speculation is that the coupled glutamate flux occurs within a glutamate transporter monomer, whereas the anion-conducting pathway is formed in the space among the monomers in a pentameric structure (41). If the latter idea is correct, one way to identify the chloride-conducting pathway may be to search for residues that participate in the formation of interfaces between monomers.

Two groups have also documented that sulfhydryl modification of cysteine replacement mutants of the related human glutamate transporter EAAT-1 results in the elimination of the coupled flux but not the uncoupled process. In one report (42), the cysteine was introduced at a position corresponding to residue 417 of EAAC-1, and in the other report (43), the cysteine replacement was at a position corresponding to EAAC-1 residue 420.

Acknowledgments—We thank Dr. Hans Peter Larsson for helpful discussions and Beryl Levene for expert secretarial assistance.

REFERENCES

1. Kanner, B. I., and Schuldiner, S. (1987) *CRC Crit. Rev. Biochem.* **22,** 1–38
2. Nicholls, D., and Attwell, D. (1990) *Trends Pharmacol. Sci.* **11,** 462–468
3. Zerangue, N., and Kavanaugh, M. P. (1996) *Nature* **383,** 634–637
4. Rothstein, J. D., Dykes Hoberg, M., Pardo, C. A., Bristol, L. A., Jin, L., Kuncl, R. W., Kanai, Y., Hediger, M. A., Wang, Y., Schielke, J. P., and Welty, D. F. (1996) *Neuron* **16,** 675–686
5. Tanaka, K., Watase, K., Manabe, T., Yamada, K., Watanabe, M., Takahashi, K., Iwama, H., Nishikawa, T., Ichihara, N., Kikuchi, T., Okuyama, S., Kawashima, N., Hori, S., Takimoto, M., and Wada, K. (1997) *Science* **276,**

1699–1702
6. Mennerick, S., and Zorumski, C. F. (1994) *Nature* **368,** 59–62
7. Tong, G., and Jahr, C. E. (1994) *Neuron* **13,** 1195–1203
8. Otis, T. S., Wu, Y. C., and Trussell, L. O. (1996) *J. Neurosci.* **16,** 1634–1644
9. Diamond, J. S., and Jahr, C. E. (1997) *J. Neurosci.* **17,** 4672–4687
10. Kanner, B. I., and Sharon, I. (1978) *Biochemistry* **17,** 3949–3953
11. Brew, H., and Attwell, D. (1987) *Nature* **327,** 707–709
12. Wadiche, J. I., Arriza, J. L., Amara, S. G., and Kavanaugh, M. P. (1995) *Neuron* **14,** 1019–1027
13. Kanner, B. I., and Bendahan, A. (1982) *Biochemistry* **21,** 6327–6330
14. Pines, G., and Kanner, B. I. (1990) *Biochemistry* **29,** 11209–11214
15. Kavanaugh, M. P., Bendahan, A., Zerangue, N., Zhang, Y., and Kanner, B. I. (1997) *J. Biol. Chem.* **272,** 1703–1708
16. Levy, L. M., Warr, D., and Attwell, D. (1998) *J. Neurosci.* **18,** 9620–9628
17. Pines, G., Danbolt, N. C., Bjoras, M., Zhang, Y., Bendahan, A., Eide, L., Koepsell, H., Storm-Mathisen, J., Seeberg, E., and Kanner, B. I. (1992) *Nature* **360,** 464–467
18. Storck, T., Schulte, S., Hofmann, K., and Stoffel, W. (1992) *Proc. Natl. Acad. Sci. U. S. A.* **89,** 10955–10959
19. Kanai, Y., and Hediger, M. A. (1992) *Nature* **360,** 467–471
20. Fairman, W. A., Vandenberg, R. J., Arriza, J. L., Kavanaugh, M. P., and Amara, S. G. (1995) *Nature* **375,** 599–603
21. Arriza, J. L., Eliasof, S., Kavanaugh, M. P., and Amara, S. G. (1997) *Proc. Natl. Acad. Sci. U. S. A.* **94,** 4155–4160
22. Grunewald, M., Bendahan, A., and Kanner, B. I. (1998) *Neuron* **21,** 623–632
23. Slotboom, D. J., Sobczak, I., Konings, W. N., and Lolkema, J. S. (1999) *Proc. Natl. Acad. Sci. U. S. A.* **95,** 14282–14287
24. Grunewald, M., and Kanner, B. I. (2000) *J. Biol. Chem.* **275,** 9684–9689
25. Seal, R. P., Leighton, B. H., and Amara, S. G. (2000) *Neuron* **25,** 695–706
26. Zhang, Y., Bendahan, A., Zarbiv, R., Kavanaugh, M. P., and Kanner, B. I. (1998) *Proc. Natl. Acad. Sci. U. S. A.* **95,** 751–755
27. Zhang, Y., and Kanner, B. I. (1999) *Proc. Natl. Acad. Sci. U. S. A.* **96,** 1710–1715
28. Borre, L., and Kanner, B. I. (2001) *J. Biol. Chem.* **276,** 40396–40401
29. Bendahan, A., Armon, A., Madani, N., Kavanaugh, M. P., and Kanner, B. I. (2000) *J. Biol. Chem.* **275,** 37436–37442
30. Wadiche, J. I., Amara, S. G., and Kavanaugh, M. P. (1995) *Neuron* **15,** 721–728
31. Pines, G., Zhang, Y., and Kanner, B. I. (1995) *J. Biol. Chem.* **270,** 17093–17097
32. Kunkel, T. A., Roberts, J. D., and Zakour, R. A. (1987) *Methods Enzymol.* **154,** 367–382
33. Fuerst, R., Niles, E. G., Studier, F. W., and Moss, B. (1986) *Proc. Natl. Acad. Sci. U. S. A.* **83,** 8122–8126
34. Wadiche, J. I., and Kavanaugh, M. P. (1998) *J. Neurosci.* **18,** 7650–7661
35. Otis, T. S., and Kavanaugh, M. P. (2000) *J. Neurosci.* **20,** 2749–2757
36. Grewer, C., Watzke, N., Wiessner, M., and Rauen, T. (2000) *Proc. Natl. Acad. Sci. U. S. A.* **97,** 9706–9711
37. Auger, C., and Attwell, D. (2000) *Neuron* **28,** 547–558
38. Watzke, N., Rauen, T., Bamberg, E., and Grewer, C. (2000) *J. Gen. Physiol.* **116,** 609–621
39. Vandenberg, R. J., Mitrovic, A. D., and Johnston, G. A. (1998) *Mol. Pharmacol.* **54,** 189–196
40. Mitrovic, A. D., Plesko, F., and Vandenberg, R. J. (2001) *J. Biol. Chem.* **276,** 26071–26076
41. Eskandari, S., Kreman, M., Kavanaugh, M. P., Wright, E. M., and Zampighi, G. A. (2000) *Proc. Natl. Acad. Sci. U. S. A.* **95,** 8641–8646
42. Seal, R. P., Shigeri, Y., Eliasof, S., Leighton, B. H., and Amara, S. G. (2001) *Proc. Natl. Acad. Sci. U. S. A.* **98,** 15324–15329
43. Ryan, R. M., and Vandenberg, R. J. (2002), *J. Biol. Chem.* **277,** 13494–13500

Dynamic Equilibrium between Coupled and Uncoupled Modes of a Neuronal Glutamate Transporter

Lars Borre, Michael P. Kavanaugh and Baruch I. Kanner

J. Biol. Chem. 2002, 277:13501-13507.
doi: 10.1074/jbc.M110861200 originally published online January 31, 2002
